

Evolution of Magnetic and Superconducting States in UCoGe With Fe and Ni Substitution

J. J. Hamlin, R. E. Baumbach, K. Huang, M. Janoschek, N. Kanchanavatee, D. A. Zocco, and M. B. Maple

Department of Physics, University of California, San Diego
La Jolla, CA 92122, U.S.A.

ABSTRACT

The very small number of known ferromagnetic superconductors places the study of such compounds at the frontier of superconductivity research. Recently, UCoGe has emerged as a new member of the class of materials exhibiting coexistence of ferromagnetism and superconductivity (Curie temperature $T_{\text{Curie}} = 3$ K; superconducting critical temperature $T_s = 0.8$ K). This compound has generated much excitement, in part because it has been proposed that the superconductivity derives from spin triplet pairing mediated by ferromagnetic interactions. Therefore, a key question is how changes in the magnetic state of UCoGe affect the superconducting properties. We have carried out a comprehensive study of the $\text{UCo}_{1-x}\text{Fe}_x\text{Ge}$ and $\text{UCo}_{1-x}\text{Ni}_x\text{Ge}$ series of compounds across the entire range of composition $0 \leq x \leq 1$. We report the results of x-ray diffraction, electrical resistivity, and magnetization measurements to elucidate the magnetic and superconducting phase diagram of the U[Fe, Co, Ni]Ge system. Substitution of either Ni or Fe into UCoGe initially results in an increase in the Curie temperature. At higher dopant concentrations (x), the ferromagnetic state crosses over to paramagnetism in $\text{UCo}_{1-x}\text{Fe}_x\text{Ge}$ and antiferromagnetism in $\text{UCo}_{1-x}\text{Ni}_x\text{Ge}$.

INTRODUCTION

Materials such as ErRh_4B_4 [20,21,1] and HoMo_6S_8 [22,2], which display the coexistence of superconductivity (SC) and ferromagnetism (FM), have been known for over three decades. In these two compounds, the latter compounds T_{Curie} lies below T_s and the superconductivity vanishes at a second, lower critical temperature $T_s' < T_{\text{Curie}}$. Within the temperature interval between T_s' and T_{Curie} , the ferromagnetism and superconductivity coexist macroscopically (in a spatially inhomogeneous manner), whereas a new sinusoidally-modulated state with a wavelength ~ 100 Å and superconductivity coexist microscopically (within the same volume element) [3]. In contrast, the recently discovered uranium-based compounds UCoGe [8], UGe_2 (under pressure) [4], UIr (under pressure) [5], and URhGe [6] appear to exhibit the microscopic coexistence of superconductivity and itinerant electron ferromagnetism. Such a coexistence is intriguing since, in a conventional superconductor, the large internal field generated by the ferromagnetic order would be expected to destroy the superconducting state by breaking the spin-singlet Cooper pairs [7]. It is thus often suggested that the superconducting electrons in such compounds may pair in triplet states, mediated by critical fluctuations associated with a ferromagnetic quantum critical point (QCP) [8-10].

A key question for any magnetic superconductor is how changes in the magnetic state effect the superconducting critical temperature. For UCoGe, both chemical substitution and pressure have been used to address this question. Upon isovalent doping of Si for Ge ($\text{UCoGe}_{1-x}\text{Si}_x$), both T_s and T_{Curie} decrease until they both vanish simultaneously for $x \geq 0.12$ [9]. This result strongly suggests an intimate link between the two states, wherein the superconductivity is

enhanced by the presence of ferromagnetic order. In contrast, under pressure, T_{Curie} decreases and T_s initially increases [18,19]. Near 1 GPa, T_{Curie} is suppressed to zero temperature and T_s passes through a broad maximum of ~ 1 K. A similar negative correlation between T_{Curie} and T_s was found for small (1% and 5%) replacements of Co with Fe, Ru, and Ni, where the magnetic ordering temperature increased and the superconductivity was rapidly suppressed [11].

In this manuscript, we report X-ray diffraction, electrical resistivity, and magnetization measurements on polycrystalline $\text{UCo}_{1-x}\text{Fe}_x\text{Ge}$ and $\text{UCo}_{1-x}\text{Ni}_x\text{Ge}$ samples for x spanning the entire range from 0 - 1. The motivation for this study was to examine the evolution of the superconducting and magnetic critical temperatures on tuning from weak itinerant ferromagnet UCoGe to either paramagnetic UFeGe or antiferromagnetic (AFM) UNiGe .

Both UCoGe and UNiGe crystallize in the orthorhombic TiNiSi structure. UFeGe only adopts the orthorhombic TiNiSi structure above ~ 500 °C and, below this temperature, exhibits a monoclinic distortion of the TiNiSi structure [12]. UFeGe remains paramagnetic down to the lowest temperatures measured [13]. UNiGe develops incommensurate AFM below 50 K and, below 42 K, commensurate AFM order sets in [14]. Low temperature measurements down to 1.5 K and 0.4 K show no evidence for superconductivity in UFeGe [12] and UNiGe [15], respectively.

EXPERIMENT

Undoped and doped polycrystalline samples of $\text{UCo}_{1-x}\text{Fe}_x\text{Ge}$ and $\text{UCo}_{1-x}\text{Ni}_x\text{Ge}$ (where $0 \leq x \leq 1$) were synthesized by arc melting the pure elements in stoichiometric ratios, under an argon atmosphere. The boules were flipped over several times and re-melted in order to insure homogeneous mixing of the starting elements. As-grown samples were cut in half using a diamond wheel saw, and half of each boule was annealed in vacuum at 900 °C for 10 days. The chemical compositions were confirmed by energy dispersive x-ray (EDX). Powder X-ray diffraction data was collected with a Bruker D8 x-ray diffractometer utilizing $\text{Cu K}\alpha$ radiation.

Magnetization measurements were performed in a Quantum Design (MPMS) SQUID magnetometer for $2 \text{ K} \leq T \leq 300 \text{ K}$ and magnetic fields up to 7 tesla. Four-wire electrical resistivity measurements utilized a Linear Research LR-700 ac-resistance bridge operating at 16 Hz. Electrical resistivity of $\text{UCo}_{1-x}\text{Fe}_x\text{Ge}$ with nominal concentrations $x = 0, 0.025, 0.1, 0.15, 0.175, 0.2, 0.3$, and 0.4 and $\text{UCo}_{1-x}\text{Ni}_x\text{Ge}$ with $x = 0.05, 0.52$, and 0.56 were measured down to ~ 0.05 K in an Oxford Kelvinox-300 ^3He - ^4He dilution refrigerator.

RESULTS

Analysis of the powder X-ray diffraction patterns shows that the orthorhombic TiNiSi crystal structure exists across the entire Fe-doping series. However, the iron-rich $\text{UCo}_{0.2}\text{Fe}_{0.8}\text{Ge}$ and $\text{UCo}_{0.1}\text{Fe}_{0.9}\text{Ge}$ samples exhibit significant concentrations of an unidentified impurity phase. Post annealing of the $\text{UCo}_{1-x}\text{Fe}_x\text{Ge}$ samples, as described above, results in an increased fraction of this impurity phase in the $x < 0.8$ samples. For this reason, we present data for the unannealed $\text{UCo}_{1-x}\text{Fe}_x\text{Ge}$ samples.

The $\text{UCo}_{1-x}\text{Ni}_x\text{Ge}$ samples exhibit the orthorhombic TiNiSi structure across the entire doping range $x = 0 - 1$. We present data for the annealed Ni-doped samples, although no significant differences between annealed and unannealed samples could be found in the diffraction patterns.

Figures 1 and 2 show the lattice constants and cell volume for both doped and undoped samples. The results for as-grown and annealed roughly agree for all dopings except undoped UCoGe and the $x = 0.025$ Fe-doped samples where the as-grown samples show slightly larger lattice constants.

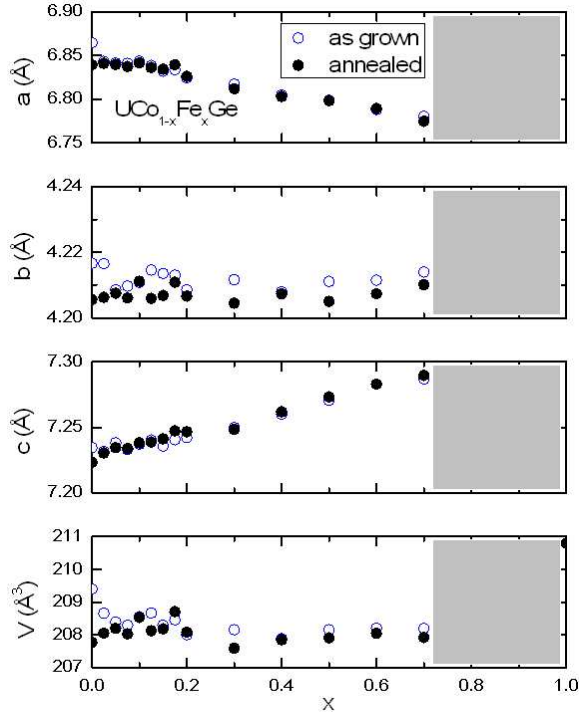


Figure 1: Lattice constants and volume for both as-grown and annealed $\text{UCo}_{1-x}\text{Fe}_x\text{Ge}$. The grey regions indicate mixed-phase samples.

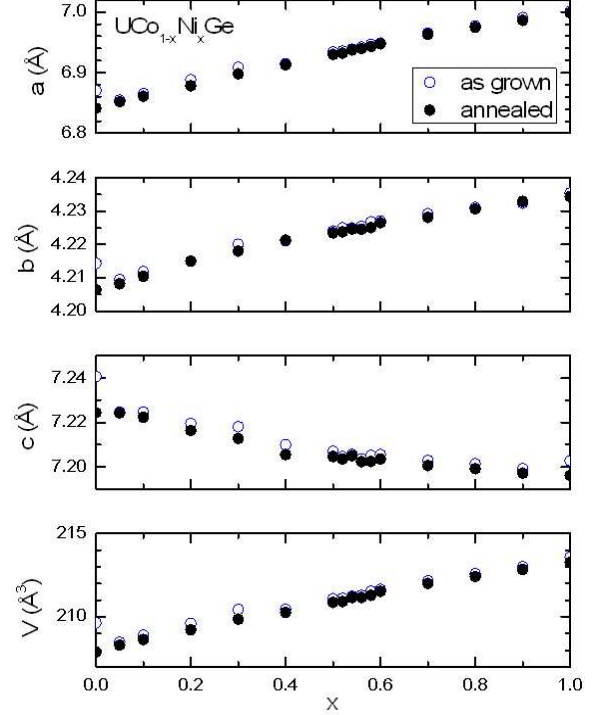


Figure 2: Lattice constants and volume for both as-grown and annealed $\text{UCo}_{1-x}\text{Ni}_x\text{Ge}$.

Figures 3 and 4 show magnetization versus temperature for Fe- and Ni- doped samples, respectively. The data were measured on cooling from room temperature in 10 Oe (or 100 Oe in the inset of the middle panel of Figure 4). Upon increasing Fe concentrations, T_{Curie} increases up to ~ 10 K at $x=0.075$ and then falls at higher concentrations. For Fe concentrations $x \geq 0.3$, T_{Curie} is suppressed below the measurement limit of ~ 2 K. A rough extrapolation of the trend would suggest that T_{Curie} is driven to zero temperature slightly above $x = 0.2$.

Ni-doped samples with $x \leq 0.4$ (upper panel of Figure 4) show a clear ferromagnetic characteristic while samples with $x \geq 0.58$ (lower panel of Figure 4) display a peak in the magnetization typical of AFM ordering. For samples in the intermediate doping range $x = 0.5 - 0.56$ (middle panel of Figure 4) the exact nature of the magnetic ordering is difficult to unambiguously determine from M versus T data alone. In 10 Oe, the magnetization of these samples saturates at low temperatures, whereas in 100 Oe (inset of Figure 4), the magnetization passes through a weak maximum suggesting AFM behavior. Upon doping with Ni, T_{Curie} initially increases and passes through a maximum of ~ 26 K near $x = 0.2$. The ordering temperature then evolves through a shallow minimum near $x = 0.4$ before crossing over to AFM behavior. In the highly Ni-doped regime, T_{N} reaches a maximum of ~ 44 K near $x = 0.9$.

From these magnetization curves, the critical temperatures for magnetic ordering have been determined and plotted versus dopant concentration in Figures 5 and 6. For the FM samples, we estimate T_{Curie} by extrapolating the magnetization near the transition to zero. For the AFM samples, the Néel temperature T_N is determined by the peak in magnetization. Ni-doped samples in the region between $x = 0.5 - 0.56$ (labeled “crossover regime” in Figure 6) could exhibit magnetic phase separation, glassy behavior, or some other form of complex magnetism. Further measurements are necessary to distinguish between these possibilities.

Of the samples for which we measured the low temperature electrical resistivity, only undoped UCoGe ($T_s \sim 0.68$ K) and UCo_{0.975}Fe_{0.025}Ge ($T_s \sim 0.56$ K) displayed superconductivity. The superconducting transition of the Fe-doped $x = 0.025$ exhibited only ~ 50 % of a full drop to zero resistance and could be due to a small phase fraction of undoped UCoGe. The rapid suppression of T_s is in agreement with the results of Pospíšil *et al.* [11], who found that small concentrations of Fe or Ni significantly enhance the ferromagnetism and are sufficient to destroy the superconductivity. Superconductivity also appears to be absent in the Fe-doped samples near $x = 0.2$, the critical concentration for the destruction of the ferromagnetic state. Further details of our electrical resistivity measurements will be reported elsewhere [16].

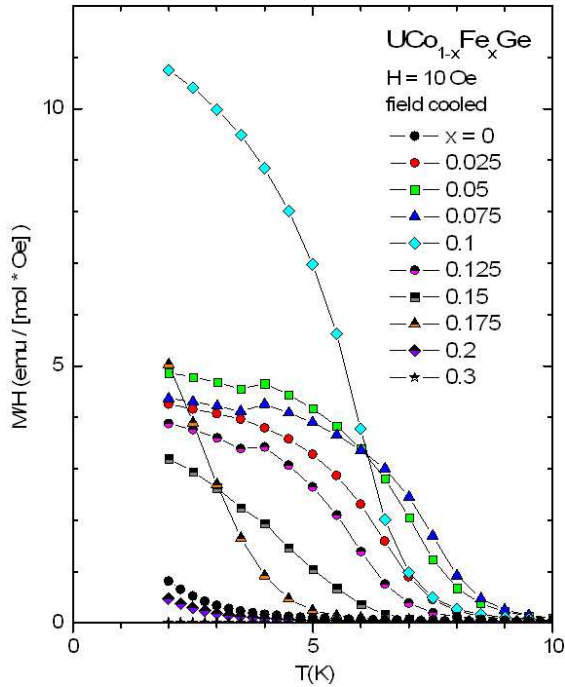


Figure 3: Magnetic susceptibility (M/H), measured in a field of 10 Oe, for UCo_{1-x}Fe_xGe.

DISCUSSION

An interesting aspect of the present work is the possibility of a critical point near $x = 0.2$ in the phase diagram of UCo_{1-x}Fe_xGe. The superconductivity in UCoGe is thought to derive from its proximity to a ferromagnetic quantum critical point. Thus, one may ask why similar

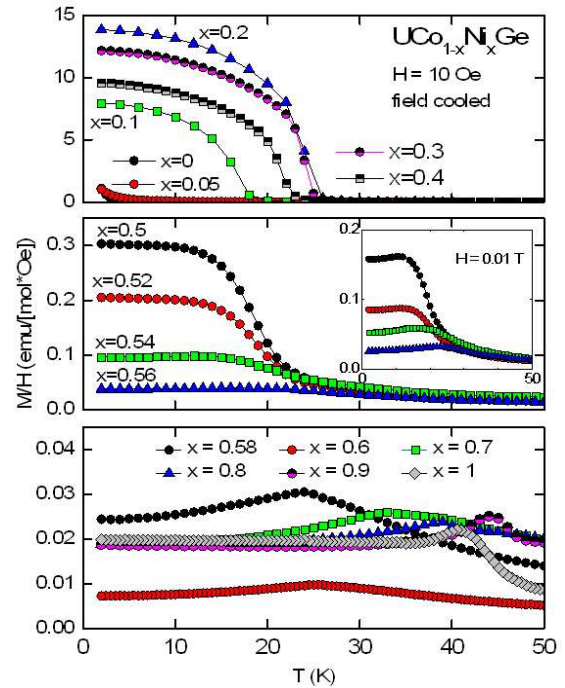


Figure 4: Magnetic susceptibility (M/H), measured in a field of 10 Oe (100 Oe in inset), for UCo_{1-x}Ni_xGe. The upper, middle, and lower panels show results for low, intermediate, and high doping values, respectively.

superconductivity is not found near the $\text{UCo}_{0.8}\text{Fe}_{0.2}\text{Ge}$ concentration. It is often suggested that spin-triplet superconductivity is only stable in extremely high quality crystals with long mean-free-paths. The known materials which appear to exhibit microscopic coexistence of ferromagnetism and superconductivity are undoped, stoichiometric compounds. If the superconductivity in UCoGe is indeed spin-triplet in nature, the lack of superconductivity near the $\text{UCo}_{0.8}\text{Fe}_{0.2}\text{Ge}$ concentration may, therefore, be due to doping-induced disorder. However, in the case UGe_2 , which has also been proposed as a spin-triplet superconductor, superconductivity is found in polycrystalline samples with mean-free-paths comparable to the superconducting coherence length [17]. Efforts are currently underway to study the region near $\text{UCo}_{0.8}\text{Fe}_{0.2}\text{Ge}$ with finer doping increments, in high quality single- and poly- crystalline samples, in order to investigate whether non-Fermi-liquid behavior and/or superconductivity emerge near this ferromagnetic critical point.

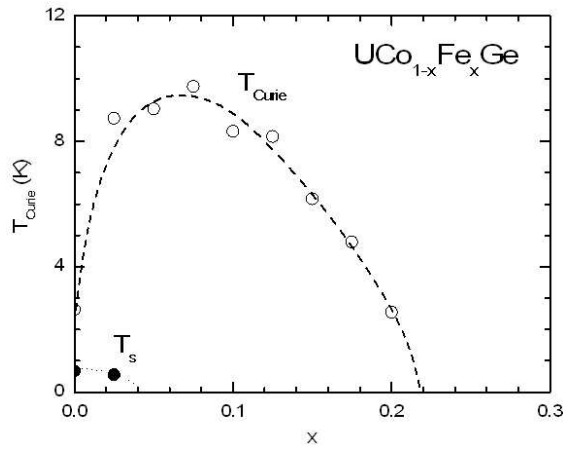


Figure 6: Temperature T vs. composition x phase diagram of $\text{UCo}_{1-x}\text{Fe}_x\text{Ge}$. Dashed lines are a guide to the eye.

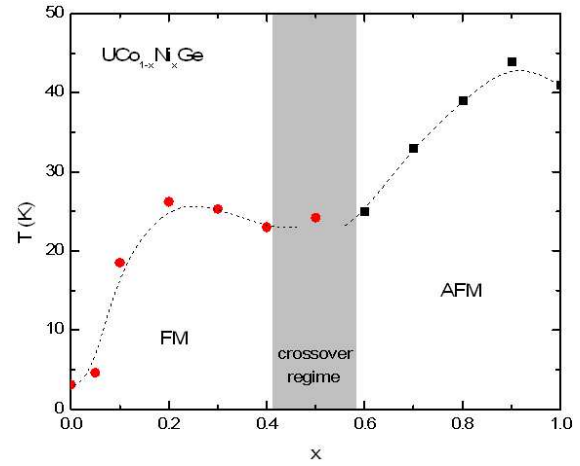


Figure 5: Temperature T vs. composition x phase diagram of $\text{UCo}_{1-x}\text{Ni}_x\text{Ge}$. The dashed line is a guide to the eye.

ACKNOWLEDGMENTS

Sample synthesis and basic characterization were sponsored by the U.S. Department of Energy (DOE) under grant No. DE-FG02-04ER46105 and acquisition of crystal growth equipment was sponsored by the US DOE through grant No. DE FG02-04ER46178. Low temperature dilution refrigerator measurements were supported by the National Science Foundation under Grant No. DMR 0802478.

REFERENCES

1. S. K. Sinha, G. W. Crabtree, D. G. Hinks, and H. Mook, Phys. Rev. Lett. **48**, 950, 1982
2. J. W. Lynn, G. Shirane, W. Thomlinson, and R. N. Shelton, Phys. Rev. Lett. **46**, 368, 1981
3. M. B. Maple, R. E. Baumbach, J. J. Hamlin, D. A. Zocco, B. J. Taylor, N. P. Butch, J. R. Jeffries, S. T. Weir, B. C. Sales, D. Mandrus, M. A. McGuire, A. S. Sefat, R. Jin, Y. K. Vohra, J. -H. Chu, and I. R. Fisher, Physica B **404**, 2924, 2009

4. S. S. Saxena, K. Ahilan, P. Agarwal, F. M. Grosche, R. K. Haselwimmer, M. Steiner, E. Pugh, I. R. Walker, S. R. Julian, P. Monthoux, G. G. Lonzarich, A. D. Huxley, I. Sheikin, D. Braithwaite, and J. Flouquet, *Nature (London)* **406**, 587, 2000
5. T. Akazawa, H. Hidaka, T. Fujiwara, T. C. Kobayashi, E. Yamamoto, Y. Haga, R. Settai, and Y. Onuki: *J. Phys., Condens. Matter* **16**, L29, 2004
6. D. Aoki, A. D. Huxley, E. Ressouche, D. Braithwaite, J. Flouquet, J. P. Brison, E. Lhotel, and C. Paulsen, *Nature (London)* **413**, 613, 2001
7. N. F. Berk, and J. R. Schrieffer, *Phys. Rev. Lett.* **17**, 433, 1966
8. N. T. Huy, A. Gasparini, D. E. de Nijs, Y. Huang, J. C. P. Klaasse, T. Gortenmulder, de A. Visser, A. Hamann, T. Görlach, and H. v. Löhneysen, *Phys. Rev. Lett.* **99**, 067006, 2007
9. D. E. de Nijs, N. T. Huy, and A. de Visser, *Phys. Rev. B.* **77**, 140506, 2008
10. N. T. Huy, and A. de Visser, *Solid State Commun.* **149**, 703, 2009
11. J. Pospíšil, J. Poltírová Vejpravová, M. Diviš, and V. Sechovský, *J. Appl. Phys.* **105** 07E114, 2009
12. F. Canepa, P. Manfrinetti, M. Pani, and A. Palenzona, *J. Alloys Comp.* **234**, 225, 1996
13. L. Havela, A. Kolomiets, V. Sechovský, M. Diviš, M. Richter, A. V. Andreev, *J. Mag. Magn. Mat.* **177-181**, 47, 1998
14. V. Sechovsky, L. Havela, A. Purwanto, A. C. Larson, R. A. Robinson, K. Prokeš, H. Nakotte, E. Brück, F. R. de Boer, P. Svoboda, H. Maletta, and M. Winkelmann, *J. Alloys Compounds* **213-214**, 536, 1994
15. I. H. Hagmusa, J. C. P. Klaasse, E. Brück, K. Prokeš, F. R. de Boer, and H. Nokotte, *J. Appl. Phys.* **81**, 4157, 1997
16. *manuscript in preparation*
17. E. D. Bauer, R. P. Dickey, V. S. Zapf, and M. B. Maple, *J. Phys.: Condens. Matter* **13**, L759, 2001
18. E. Hassinger, D. Aoki, G. Knebel, and J. Flouquet, *J. Phys. Soc. Japan* **77**, 073703, 2008
19. E. Slooten, T. Naka, A. Gasparini, Y. K. Huang, and A. de Visser, *Phys. Rev. Lett.* **103**, 097003, 2009
20. W. A. Fertig, D. C. Johnston, E. DeLong, R. W. McCallum, M. B. Maple, and B. T. Matthias, *Phys. Rev. Lett.* **38**, 987, 1977
21. D. E. Moncton, D. B. McWhan, J. Eckert, G. Shirane, and W. Thomlinson, *Phys. Rev. Lett.* **39**, 1164, 1977
22. M. Ishikawa, and Ø. Fischer, *Solid State Comm.* **23**, 37, 1977